

## Inelastic Pion Double Charge Exchange on $^{16}\text{O}$ at 240 MeV

R. E. Mischke,<sup>(a)</sup> A. Blomberg, P. A. M. Gram,<sup>(a)</sup> J. Jansen,<sup>(b)</sup> and J. Zichy  
*Swiss Institute for Nuclear Research, 5234 Villigen, Switzerland*

and

J. Bolger, E. Boschitz, C. H. Q. Ingram,<sup>(c)</sup> and G. Pröbstle  
*Kernforschungszentrum und Universität Karlsruhe, D-7500 Karlsruhe, Federal Republic of Germany*  
 (Received 29 January 1980)

The deep-inelastic double-charge-exchange reaction  $^{16}\text{O}(\pi^+, \pi^-)$  has been measured at  $50^\circ$ ,  $85^\circ$ , and  $130^\circ$  with 240-MeV incident pions. The doubly differential cross section is peaked at low outgoing pion energies, as is expected from a double-scattering process, and is nearly isotropic. The integrated cross section is  $5.8 \pm 0.9$  mb. The shape of the differential cross section suggests that the low-energy tail in  $^{16}\text{O}(\pi^+, \pi^{+'})$  scattering at the same energy also arises from double scattering.

PACS numbers: 25.80.+f

A recent experiment<sup>1</sup> on the reaction  $^{16}\text{O}(\pi^+, \pi^{+'})$  at pion energies from 115 to 240 MeV has indicated that a substantial fraction of this cross section is the result of single quasifree pion-nucleon collisions within the nucleus. The doubly differential cross section  $d\sigma/d\Omega dE$  displays a large quasifree peak, but it is not possible to distinguish between single- and multiple-collision processes in such an experiment.

Pion double charge exchange, however, cannot proceed via a single pion-nucleon interaction within the nucleus but must involve at least two nucleons in order to conserve charge. In view of the apparent dominance of the  $(\pi^+, \pi^{+'})$  quasifree reaction, it is supposed that the dominant pion double-charge-exchange mechanism is two single-charge-exchange collisions:  $\pi^+n \rightarrow \pi^0p$  followed by  $\pi^0n \rightarrow \pi^-p$ .

A ratio of 26:1 between cross sections for double scattering of the incident pion  $(\pi^+, \pi^{+'})$  and double charge exchange can be calculated from isospin arguments if it is assumed that both scatterings occur at the  $\Delta(1232)$  resonance and that the resultant cross sections are approximately isotropic. Thus in nuclei we expect the double-charge-exchange cross section to be a rather small fraction of the total reaction cross section. However, because it is specific to multiple pion-nucleon interactions, the shape and magnitude of the inelastic double-charge-exchange cross section is an important element in understanding pion-nucleus dynamics.

This experiment measures the continuum spectrum of pions from double charge exchange down to  $T_\pi = 35$  MeV. Early pion double-charge-exchange experiments<sup>2-5</sup> were attempts to measure double isobaric analog transitions. Some da-

ta were obtained on inelastic scattering to the continuum, but the range of outgoing pion energy was limited to the high-energy region.<sup>4</sup> Recent double-charge-exchange measurements<sup>6-8</sup> were similarly interested primarily in bound final states or again had limited coverage of the outgoing pion energy.<sup>9</sup>

The experiment was performed at the Swiss Institute for Nuclear Research using the pion spectrometer SUSI.<sup>10</sup> A flux of 240-MeV pions of intensity  $2 \times 10^7 \pi^+/\text{sec}$  was incident on a water target 1.3 g/cm<sup>2</sup> thick. The spectrometer has a large momentum and angular acceptance; the included ranges of angles and momenta were restricted to regions where the apparatus exhibits uniform acceptance (10 msr and 20% in momentum). The spectrum of scattered pion energies was covered in six steps of the spectrometer field strength over the range from  $T_\pi = 35$  to 250 MeV. Cross sections were measured at laboratory angles of  $50^\circ$ ,  $85^\circ$ , and  $130^\circ$  with an acceptance of  $\pm 5^\circ$ .

The spectrometer is a vertically bending quadrupole-double-dipole array. The entrance quadrupole focuses in the horizontal plane. Multiwire proportional chambers  $C_4$  and  $C_5$  are placed on either side of the quadrupole to define the trajectories of particles entering the system. A scintillator  $S_3$  accompanies  $C_5$ . Two more chambers  $C_6$  and  $C_7$  along with a scintillator  $S_4$  define trajectories which cross the focal plane. The system was triggered by a coincidence  $S_3 \cdot S_4$  and an incident  $\pi^+$ . Counter  $S_4$  also measured particle time of flight through the spectrometer, corrected for path length, with a resolution of 1 ns full width at half maximum.

The data analysis concentrated on rejection of

backgrounds to elicit a clean scattered- $\pi^-$  signal and reduction of systematic errors. Analysis of trajectories rejected most muons resulting from pions which decayed in the spectrometer. Several corrections were applied to the data. A correction based on the energy and path length of surviving pions was made for pions decaying in the spectrometer. The correction included an allowance for accepted events in which the pion had decayed but not rejected by trajectory analysis. The wire chambers suffered from two kinds of inefficiency for which corrections were made: (1) the inefficiency due to a chamber failing to detect a particle, and (2) an effective inefficiency whenever more than one hit appeared in a chamber plane rendering trajectory reconstruction impossible. For chambers  $C_6$  and  $C_7$  the hardware inefficiency was  $\sim 0.15$  per chamber, but multiple-hit inefficiency was small, while for chambers  $C_4$  and  $C_5$  the hardware inefficiency was 0.01 but the analysis inefficiency was between 0.08 and 0.20 depending on angle and momentum. This momentum dependence is not understood and is included as a possible systematic error.

The incident pion flux was measured with a counter in the beam. The observed number of counts was multiplied by a factor of 1.18 (determined from the pulse-height distribution in the beam counter) to account for beam pulses which contained two pions within the electronics resolving time. The effective solid angle of the spectrometer was determined from elastic scattering of  $\pi^+$  from protons in the target. This effective solid angle is momentum dependent, as a result of multiple scattering. The value at 35 MeV is  $0.80 \pm 0.12$  of that at high momentum; this is the dominant uncertainty in the normalization.

At the lowest pion energies ( $T_{\pi^-} < 100$  MeV), there is a contribution from pion production; i.e.,  $\pi^+ + {}^{16}\text{O} \rightarrow \pi^+ \pi^- X$ . The only measurement of this cross section in nuclei is  $\sigma_T \sim 150 \mu\text{b}$  on emulsion nuclei.<sup>11</sup> The measured cross section for  $\pi^- p \rightarrow \pi^+ \pi^- n$  is  $100 \mu\text{b}$ .<sup>12</sup> These results are consistent if the cross section in nuclei is strongly suppressed by Pauli blocking. Since the differential cross section for production is peaked at or below the cutoff of this experiment ( $T_{\pi^-} = 35$  MeV), with  $\sigma_T = 150 \mu\text{b}$  the maximum value is  $\sim 0.34 \mu\text{b}/(\text{sr MeV})$ . This implies a correction to our integrated cross section of only 3%.

The differential cross sections are presented in Fig. 1.<sup>13</sup> The errors shown are statistical. The momentum-dependent normalization uncertainties are correlated and decrease from  $\pm 13\%$

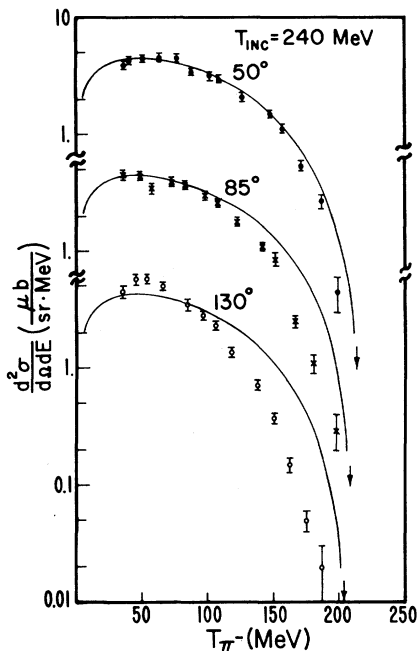


FIG. 1. Doubly differential double-charge-exchange cross sections  ${}^{16}\text{O}(\pi^+, \pi^-)$  vs laboratory kinetic energy of outgoing  $\pi^-$ . The solid lines are phase space from  $\pi^+ + {}^{16}\text{O} \rightarrow \pi + (A=14) + N + N$ . The arrows indicate the end point of the spectrum from  $\pi^+ + {}^{16}\text{O} \rightarrow \pi^- + {}^{16}\text{Ne}_{g.s.}$ .

to  $\pm 6\%$  at 200 MeV. The total cross section obtained by integrating over pion energy and angle is  $5.8 \pm 0.9$  mb. The shape of the cross section in the region  $T_{\pi^-} = 0$  to 35 MeV was approximated by a phase-space calculation. The error includes an allowance of  $\pm 5\%$  for uncertainty in the shape.

Note that the differential cross section is rather isotropic and peaked around 50 MeV  $\pi^-$  energy. This is expected from the kinematics of multiple quasifree scattering since a 240-MeV incident pion loses typically 50–150 MeV to the recoil nucleon in each scatter.<sup>1</sup> The angular dependence in the high-energy region is mostly an effect of recoil, since the cross sections are presented in the laboratory system. The end points of the spectra are indicated by the location of the  ${}^{16}\text{Ne}$  ground state in the reaction  $\pi^+ + {}^{16}\text{O} \rightarrow \pi^- + {}^{16}\text{Ne}_{g.s.}$ . These end points are 213.5, 208, and 203.5 MeV at  $50^\circ$ ,  $85^\circ$ , and  $130^\circ$ , respectively.

At the high-energy end of the spectra, there are no valid events for  $T_{\pi^-} > 190$  MeV at  $130^\circ$  and for  $T_{\pi^-} > 195$  MeV at  $85^\circ$ . There is one event above  $T_{\pi^-} = 205$  MeV at  $50^\circ$ . The cross-section limit integrated from the listed energy to the end point is  $< 60$  nb/sr at  $85^\circ$  and  $130^\circ$  and  $50 \pm 50$  nb/sr at  $50^\circ$ .

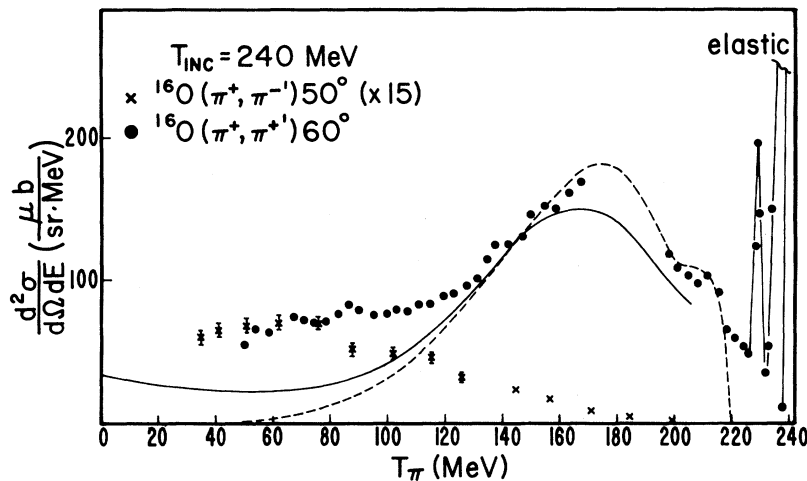


FIG. 2. Double-charge-exchange cross section at  $50^\circ$  (multiplied by 15) compared with  $^{16}\text{O}(\pi^+, \pi^{+\prime})$  data at  $60^\circ$  from Ref. 1. Also shown are (arbitrarily normalized)  $^{12}\text{C}(e, e')$  data at  $60^\circ$  and  $360$  MeV from Ref. 14 (solid curve) and a single-scattering calculation from Ref. 15 (dashed curve).

In Fig. 1, the differential cross sections are compared to four-body phase space calculated for the reaction  $\pi + ^{16}\text{O} \rightarrow \pi + (A=14) + N + N$ . It is assumed that this gives a representative shape for probable multiparticle final states. The normalization of the phase-space curves was arbitrarily adjusted to "fit" the data at  $50^\circ$ . The difference in shape between data and phase space is much larger at  $130^\circ$  than at  $50^\circ$ .

These data can aid in understanding the inclusive pion-scattering spectrum. At  $240$  MeV and  $60^\circ$  the  $^{16}\text{O}(\pi^+, \pi^{+\prime})$  spectrum has a strong single-scattering peak centered near  $185$ -MeV scattered pion energy as shown in Fig. 2. The long tail extending to lower energies is presumably due to multiple scattering of the incident pion. Fairly reliable estimates of the shape due to single scattering alone can be obtained from (1) the  $360$ -MeV  $^{12}\text{C}(e, e')$  data of Mougey *et al.*<sup>14</sup> which has the same momentum transfer, and (2) a single quasi-free  $\pi^+ - ^{16}\text{O}$  scattering calculation of Thies, Horikawa, and Lenz.<sup>15</sup> The electron-scattering data start to rise at low energy because of pion production, not multiple scattering, which is unlikely for electrons. If our double-charge-exchange spectrum at  $50^\circ$  is scaled by an arbitrary factor of 15 to match the low-energy part of the spectrum, it accounts reasonably well for the excess over single scattering. Pion-production background, off-resonance scattering, and less simple processes than double quasifree scattering might all reduce the factor from the idealized value of 26.

It is hoped that our data will also prove useful in understanding double-charge-exchange processes to bound final states. There seems to be a smooth transition from our continuum measurements into the region where the bound states are observed. Direct comparisons between experiments are difficult at present because there is no overlap in targets, incident energies, or angles. Neither the double isobaric analog nor nonanalog states are satisfactorily understood.<sup>8</sup> When one considers which of the possible rare processes contribute to the bound final-state transitions, the pion-nucleus dynamics used to explain them should be consistent with the yields of inelastic double charge observed in this experiment.

We gratefully acknowledge support from Schweizerisches Institut für Nuklearforschung, the Bundesministerium für Forschung und Technologie, and the U. S. Department of Energy.

<sup>(a)</sup>Permanent address: Los Alamos Scientific Laboratory, Los Alamos, N. Mex. 87545.

<sup>(b)</sup>Present address: Lawrence Berkeley Laboratory, Berkeley, Cal. 94720.

<sup>(c)</sup>Present address: Swiss Institute for Nuclear Research, 5234 Villigen, Switzerland.

<sup>1</sup>C. H. Q. Ingram, in *Meson-Nuclear Physics-1979*, edited by E. V. Hungerford, III, AIP Conference Proceedings No. 54 (American Institute of Physics, New York, 1979), p. 455; C. H. Q. Ingram, J. Bolger, E. T. Boschitz, G. Pröbstle, J. A. Jansen, J. Zichy, P. A. M.

- Gram, R. E. Mischke, and J. Arvieux, to be published.
- <sup>2</sup>Yu. A. Batusov, S. A. Bunyatov, V. M. Sidorov, and V. A. Yarba, Joint Institute for Nuclear Research, Dubna, Report No. JINR P-1474, 1963 (unpublished), and *Yad. Fiz.* **3**, 309 (1966) [*Sov. J. Nucl. Phys.* **3**, 223 (1966)].
- <sup>3</sup>L. Gilly, M. Jean, R. Meunier, M. Spighel, J.-P. Stroot, P. Duteil, and A. Rode, *Phys. Lett.* **11**, 224 (1964).
- <sup>4</sup>P. E. Boynton, T. Devlin, J. Solomon, and V. Perez-Mendez, *Phys. Rev.* **174**, 1083 (1968).
- <sup>5</sup>C. J. Cook, M. E. Nordberg, Jr., and R. L. Burman, *Phys. Rev.* **174**, 1374 (1968).
- <sup>6</sup>R. L. Burman, M. P. Baker, M. D. Cooper, R. H. Heffner, D. M. Lee, R. P. Redwine, J. E. Spencer, T. Marks, D. J. Malbrough, B. M. Preedom, R. J. Holt, and B. Zeidman, *Phys. Rev. C* **17**, 1774 (1978).
- <sup>7</sup>K. K. Seth, H. Nann, S. Iverson, M. Kaletka, J. Hird, and H. A. Thiessen, *Phys. Rev. Lett.* **41**, 1589 (1978).
- <sup>8</sup>K. K. Seth, S. Iverson, H. Nann, M. Kaletka, J. Hird, and H. A. Thiessen, *Phys. Rev. Lett.* **43**, 1574 (1979).
- <sup>9</sup>J. Davis, J. Källne, J. S. McCarthy, R. C. Minehart, C. L. Morris, H. A. Thiessen, G. Blanpied, G. R. Burleson, K. Boyer, W. Cottingham, C. F. Moore, and C. A. Goulding, *Phys. Rev. C* **20**, 1946 (1979).
- <sup>10</sup>J.-P. Albanèse *et al.*, *Nucl. Instrum. Methods* **158**, 363 (1978).
- <sup>11</sup>Yu. A. Batusov, S. A. Bunyatov, N. Dalkhazhav, G. Ionice, E. Losnyanu, V. Mihul, V. M. Sidorov, D. Tuvdendorzh, and V. A. Yarba, *Yad. Fiz.* **9**, 378 (1969) [*Sov. J. Nucl. Phys.* **9**, 221 (1969)].
- <sup>12</sup>C. W. Bjork, S. E. Jones, T. R. King, D. M. Manley, A. T. Oyer, G. A. Rebka, Jr., J. B. Walter, R. Carawon, P. A. M. Gram, F. T. Shivley, C. A. Bordner, and E. L. Lomon, *Phys. Rev. Lett.* **44**, 62 (1980).
- <sup>13</sup>These values differ from the preliminary results presented by Ingram (Ref. 1) because of momentum-dependent corrections.
- <sup>14</sup>J. Mougey, M. Bernheim, D. Royer, D. Tarnowski, S. Turck, P. D. Zimmerman, J. M. Finn, S. Frullani, D. B. Isabelle, G. P. Capitani, E. De Sanctis, and I. Sick, *Phys. Rev. Lett.* **41**, 1645 (1978).
- <sup>15</sup>M. Thies, Y. Horikawa, and F. Lenz, private communication; M. Thies, Schweizerisches Institut für Nuklearforschung Report No. 79-007, 1979 (unpublished).

## Evidence for Nuclear Superfluidity in $^{236}\text{U}$ Isomeric- and Prompt-Fission Modes

Carlos A. Fontenla and Doracy P. Fontenla

Brookhaven National Laboratory, Upton, New York 11973  
(Received 16 August 1979)

Isomer fission in  $^{236m}\text{U}$ ,  $t_{1/2} = 125$  nsec, from  $^{235}\text{U}(d, pf)$  was compared with prompt fission  $^{235}\text{U}(n_{th}, f)$ , in twin experiments. Fine structure in the total kinetic energy, average total kinetic energy as a function of mass, and mass yield were observed in isomer fission of  $^{236m}\text{U}$ . This observation is compatible with a superfluid descent from saddle to scission points. Two peaks in the total-kinetic-energy distribution from isomer fission are observed near fragment mass 132, and this is interpreted as due to the proton-pairing effect at  $Z = 50$ .

PACS numbers: 28.85.Ge, 27.90.+b

Isomer fission tunneling from the ground state of the second well, in a double-humped fission barrier, proceeds with several megaelectronvolts less in initial excitation energy  $E^*$  (around 4 MeV less for  $^{236m}\text{U}$ , Ref. 1) than thermal-neutron-induced fission of the same nucleus. Isomer fission studies therefore provide a unique opportunity to test, in nuclei of low fissility parameter  $Z^2/A$ , the behavior attributed to shell and pairing effects over a wide range of fission fragment masses. How this behavior changes with  $E^*$  has been studied at energies at and above the fission barrier. Study of isomer fission extends the range of energies  $E^*$  below the fission barrier where the relative importance of shell and pairing effects can change. In particular, if super-

fluidity plays a role in fission, these effects should arise or be enhanced with decreasing  $E^*$ .

In the present work fine structure has been observed for isomer fission of  $^{236m}\text{U}$  in the total kinetic energy  $E_K^m$  and in the mass yield spectra as well as in the average total kinetic energy  $\langle E_K^m(\mu) \rangle$  as a function of fragment mass  $\mu$ . The same quantities obtained in a twin experiment for prompt thermal-neutron-induced fission of  $^{235}\text{U}$  do not show this structure. When only those events are selected which correspond to a heavy fragment mass near  $\mu = 132$  amu, then the  $E_K^m$  isomer spectrum has the striking feature of being split in two resolved peaks. This is an effect not previously observed in fission which may have significant implications.